Definition of the Specific Roles of Lysolecithin and Palmitic Acid in Altering the Susceptibility of Dipalmitoylphosphatidylcholine Bilayers to Phospholipase A_2[†]

Jolene B. Henshaw, Cari A. Olsen, Amelia R. Farnbach, Kelli H. Nielson, and John D. Bell*

Department of Zoology, Brigham Young University, Provo, Utah 84602

Received November 25, 1997; Revised Manuscript Received March 27, 1998

ABSTRACT: Bilayers composed of phosphatidylcholine initially resist catalysis by phospholipase A_2. However, after a latency period, they become susceptible when sufficient reaction products (lysolecithin and fatty acid) accumulate in the membrane. Temperature near the main bilayer phase transition and calcium concentration modulate the effectiveness of the reaction products. The purpose of this study was to examine the individual contributions of lysolecithin and palmitic acid to the susceptibility of dipalmitoylphosphatidylcholine vesicles and to rationalize the effects of temperature and calcium. Various fluorescent probes (Prodan, Laurdan, pyrene-labeled fatty acid, and dansyl-labeled phospholipid) were used to assess changes in the ability of the reaction products to perturb the bilayer and to affect the interactions with the enzyme. Un-ionized palmitic acid decreased bilayer polarity and perturbed the membrane surface exposing some of the Prodan to bulk water. Lysolecithin increased bilayer polarity and the rate of dipolar relaxation in response to the excited states of Laurdan and Prodan. A combination of the individual contributions of each product was observed when palmitic acid and lysolecithin were present together at low calcium, and the effects of lysolecithin dominated at high calcium. Palmitic acid, but not lysolecithin, promoted the binding of phospholipase A_2 to the bilayer surface in the absence of calcium. Lysolecithin reduced the ability of fatty acid to enhance binding apparently by altering the structure of fatty acid domains in the membrane. Furthermore, increased temperature and ionization of the fatty acid tended to cause segregation of bound phospholipase A_2 into domains poor in phospholipid content which presumably impeded bilayer hydrolysis. In contrast, un-ionized palmitic acid and lysolecithin promoted hydrolysis by augmenting a step distal to the adsorption of enzyme to the bilayer. This kinetic response to lysolecithin was calcium-dependent. A model accounting for these varied influences of the reaction products is presented.

Phospholipase A_2 (PLA_2[1]) hydrolyzes phospholipids at the sn-2 position to yield fatty acid and lysophospholipid. Physiologically, these hydrolysis products function as precursors for a variety of hormones such as prostaglandins, leukotrienes, thromboxanes, and platelet-activating factor (*1*). One form of the enzyme is secreted by several cell types and is known as the "group II" or "nonpancreatic secretory 14 kDa" enzyme. An understanding of the factors that determine the level of activity of this secretory PLA_2 is important since the enzyme appears to be responsible for some of the complications associated with inflammatory conditions and with sepsis (reviewed in refs *2* and *3*).

An emerging theme in the study of the regulation of this enzyme is that its activity is determined to a large extent by the properties of the membrane with which it interacts. In an effort to understand the physical principles that govern membrane susceptibility to PLA_2, much effort has been directed toward model systems. For example, large vesicles composed of saturated phosphatidylcholines also resist catalysis by PLA_2 (*4*). However, susceptibility can be conferred on such membranes by various interventions such as increasing the bilayer curvature (*5*, *6*) or adding various guest molecules to the bilayer such as anionic lipids (*7*−*9*), lysolecithin (*10*, *11*), or long-chain acylglycerols (*12*). The relevance of anionic lipids and lysolecithin (lyso-PC) is illustrated by the well-documented time dependence observed during the hydrolysis of large vesicles of dipalmitoylphosphatidylcholine (DPPC). When DPPC and PLA_2 are initially mixed, hydrolysis is slow due to the intrinsic resistance of the membranes to catalysis by the enzyme. However, after threshold concentrations of the reaction products, palmitic acid and lyso-PC, have accumulated in the bilayer, the rate of phospholipid hydrolysis by PLA_2 suddenly increases by one or more orders of magnitude (*11*, *13*). Both the amount of products required in the bilayer and the length of the lag phase preceding this abrupt increase in activity (tau) depend on several factors including the bilayer curvature (*14*), the

[†] This work was supported by NIH Grant GM49710.

* To whom correspondence should be addressed. Phone: (801) 378-2353. Fax: (801) 378-7499.

[1] Abbreviations: PLA_2, low molecular weight soluble phospholipase A_2; lyso-PC, monopalmitoyl lysophosphatidylcholine; DPPC, dipalmitoylphosphatidylcholine; tau, time of onset of increased PLA_2 activity; Prodan, 6-propionyl-2-(dimethylamino)naphthalene; Laurdan, 6-dodecanoyl-2-(dimethylamino)naphthalene; ADIFAB, acrylodan-labeled intestinal fatty acid-binding protein; pyrene-FA, 1-pyrenedecanoic acid; dansyl-DHPE, *N*-(5-(dimethylamino)naphthalene-l-sulfonyl)-1,2-dihexadecanoyl-*sn*-glycero-3-phosphoethanolamine; LUV, large unilamellar vesicles; GP, generalized polarization; t_m, phospholipid melting temperature; X_p, minimum mole percent of reaction product at which tau = 0.

S0006-2960(97)02880-8 CCC: $15.00
Published on Web 07/10/1998

calcium concentration (*15*), and the temperature relative to the phospholipid phase transition (*6*, *12*). These latter two factors have received particular attention, yet confusion persists regarding the mechanisms of their influence on hydrolysis kinetics (*16*).

Previous investigations have attempted to define how palmitic acid and lyso-PC affect the physical properties of the bilayer and promote increased activity of PLA_2 (*8*, *9*, *16*−*18*). Although models have been proposed to account for the various observations (*9*, *11*, *19*, *20*), most investigators appear to agree that at least two steps are involved prior to catalysis as illustrated in the following equation (*21*).

$$E + V \rightleftharpoons E_B V \overset{Ca^{2+}}{\rightleftharpoons} E_A V \qquad (1)$$

where E = enzyme, V = vesicle, E_B = enzyme bound to the vesicle surface, and E_A = enzyme bound and actively hydrolyzing lipid. In the first step, the enzyme binds to the membrane surface. The calcium-dependent second step is less well-defined. It represents phospholipid monomers from the bilayer gaining access to the active site of the enzyme. Whether this second step involves displacement of the phospholipids from the bilayer plane up into the enzyme active site, penetration of the enzyme into the bilayer, and a conformational change of the enzyme or some combination of these events remains to be fully resolved. Nevertheless, it appears clear that both steps are limiting for DPPC bilayers and that the reaction products promote susceptibility of the bilayer to PLA_2 by enhancing one or both of these steps (*8*, *9*, *11*, *16*−*18*).

A specific role for each reaction product in promoting increased susceptibility to PLA_2 has been postulated. Several workers have suggested that the negative charge of the fatty acid promotes the first step in eq 1 by increasing the adsorption of PLA_2 to the bilayer electrostatically (*8*, *9*, *22*). This effect appears to be modulated by the segregation of the fatty acid into domains within the bilayer (*8*, *23*). It has been proposed that lyso-PC enhances the second step by disrupting the structure of the bilayer surface so that substrate molecules can more easily migrate into the active site of the adsorbed enzyme (*16*, *17*). However, it is not clear whether these are the only roles of the reaction products, nor has it been established to what extent both roles apply when the two products are present in a 1:1 mixture. Therefore, we have conducted a systematic study of the effects of palmitic acid and lyso-PC alone and together on the binding and activity of PLA_2 toward DPPC bilayers and compared those results with the action of each product on relevant physical properties of the membranes. Since calcium concentration and temperature are known to influence the effectiveness of each product (*12*, *15*), they were used as experimental variables in the study. The sample pH was also varied to affect the degree of palmitic acid ionization and thus examine more closely the hypothesis that the fatty acid's primary contribution is electrostatic recruitment of the enzyme to the bilayer surface.

MATERIALS AND METHODS

DPPC and lyso-PC were purchased from Avanti Polar Lipid (Birmingham, AL). The fluorescent probes used for this work, Prodan, Laurdan, ADIFAB, 1-pyrenedodecanoic acid (pyrene-FA), and dansyl-DHPE, were purchased from Molecular Probes (Eugene, OR). Palmitic acid was obtained from Sigma. PLA_2 was purified from water moccasin (*Agkistrodon piscivorus piscivorus*) venom obtained from the Miami Serpentarium (Punta Gorda, Florida) as described (*24*) and stored as a lyophilized powder at −20 °C. The enzyme was dissolved in stock solutions of 50 mM KCl and 3 mM NaN_3 and stored at 4 °C prior to use. PLA_2 concentration was assessed by the absorbance at 280 nm (absorbance = 2.2 $mL \cdot mg^{-1} \cdot cm^{-1}$).

DPPC LUV were prepared by extrusion in 50 mM KCl, 10 mM $Na_2B_4O_7$ (pH 8.0), and 3 mM NaN_3 as previously described (*16*). The DPPC concentration was determined by phosphate assay (*25*). Prodan (0.2−0.3 mol %), Laurdan (0.1−0.3 mol %), or dansyl-DHPE (∼2 mol %) was added to the DPPC in chloroform solution prior to LUV preparation. Pyrene-FA was suspended in a 1:9 dimethylformamide/methanol solution and added to samples containing preformed vesicles at a final concentration of 1 mol %. The probe and vesicles were then allowed to equilibrate for 30 min before use to ensure incorporation of the probe into the vesicles. Observation of pyrene-FA fluorescence over time showed that the fluorescence stabilized within this time period, indicating that the probe had reached a steady state in the membrane. When used, ADIFAB was added directly to the aqueous phase of the sample. Lyso-PC was added to experimental samples of vesicles directly from a 1 mM aqueous stock containing 10% methanol, and the palmitic acid was added from a 5 or 10 mM stock dissolved in 100% methanol. Palmitic acid and lyso-PC together were suspended at a concentration of 1 mM each in 20% methanol. The final concentration of methanol did not exceed 2% (v/v) for any of the experiments and was generally much lower. Control experiments revealed that the methanol concentrations used did not interfere with the results or interpretations. The concentrations of lyso-PC and palmitic acid are expressed as a mole percent of the DPPC concentration. On the basis of published partition coefficients measured under the experimental conditions employed in this study, essentially all of the palmitic acid was partitioned in the bilayer at the concentrations used and the partitioning of lyso-PC varied from 70% at 91 μM DPPC to 93% at 500 μM DPPC (*12*, *15*). The sample volume was approximately 2 mL. The highest concentration of lyso-PC added was in Figures 9 and 10 where a 1:1 mixture of lyso-PC and palmitic acid were added up to 75 mol % of 100 μM DPPC; on the basis of the partition coefficient of lyso-PC, this translates into a bound mole fraction of 0.24 (54 μM lyso-PC partitioned, ∼75 μM palmitic acid partitioned, and 100 μM DPPC). For most experiments, the concentration of lyso-PC added was much lower. Nuclear magnetic resonance studies of vesicle morphology have suggested that preformed phosphatidylcholine vesicles tolerate the addition of at least a mole fraction of 0.4 lyso-PC without a gross change in morphology or loss of bilayer structure even though all the lyso-PC added remains in the outer leaflet of the membrane during the experiment (*26*).

Steady-state fluorescence experiments were performed with a Fluoromax (Spex Industries), GREG PC (ISS), or PC-1 (ISS) photon-counting spectrofluorometer. Monochromators, polarizers, and data acquisition were managed by computer in each instrument. Temperature was controlled

by a circulating water bath, and sample homogeneity was maintained by continuous magnetic stirring. Data were corrected for light scattering and inner filter effects when such were likely to affect the interpretation. Values for light scattering were obtained either from lifetime data as the percentage of intensity with a lifetime of 0 or by comparison to intensity measured in parallel experiments with vesicles devoid of fluorescent probes. Reaction mixtures were suspended in 50 mM KCl, 10 mM $Na_2B_4O_7$ (pH 8.0), and 3 mM NaN_3 unless otherwise noted. Calcium concentrations are indicated for the specific experiment in the text or figure legends. For ease in comparing to data previously published, calcium concentrations were chosen in the range from 1 μM to 10 mM. Solutions containing 1 μM calcium were prepared without added calcium since that present as a contaminant in the salts and buffers used gives a solution containing approximately 1 μM calcium based on spectrophotometric measurements (*15*). When the complete absence of calcium was required, experiments used an EDTA buffer containing 35 mM KCl, 10 mM EDTA, 3 mM NaN_3, and 10 mM $Na_2B_4O_7$ (pH 8.0, unless otherwise noted).

To assess the amount and mobility of bilayer water, lifetimes of Prodan and Laurdan were determined from phase modulation data obtained with an ISS phase fluorometer located at the Laboratory for Fluorescence Dynamics (an NIH National Resource Center) in Urbana, Illinois (University of Illinois). The light source was a 350 nm line obtained by doubling the frequency of the 700 nm emission from DCM dye pumped by a Nd:YAG laser (Coherent). The excitation light was also polarized at 35°. Lifetimes were measured at 10 nm wavelength increments from 410 to 530 nm with a band-pass of 16 nm using 12 frequencies ranging from 7.62 to 198.12 MHz. 2−2′−*p*-Phenylenebis(5-phenyl)-oxazole in ethanol was used as a standard (1.35 ns) for calculating lifetimes from the phase and modulation data. Data were analyzed, and the time dependence of the emission spectrum was calculated using the Globals Unlimited software available at the resource center.

Bilayer polarity and the presence of fatty acid domains were determined from Laurdan and pyrene-FA emission spectra, respectively. These spectra were analyzed quantitatively using generalized polarization (GP) (*27*). For Laurdan, the intensities at 435 and 500 were taken from emission spectra, and the GP was calculated using the following equation:

$$\mathrm{GP} = \frac{I_{435} - I_{500}}{I_{435} + I_{500}} \tag{2}$$

An increase in the value of GP represents a decrease in bilayer polarity. Pyrene-FA excimer GP values were calculated similarly using emission intensities at 396 (monomer) and 480 nm (excimer), respectively (excitation = 344 nm). We used excimer GP values for the relative excimer and monomer contributions instead of the traditional ratio since GP returns a linear representation of changes in excimer propensity. An increase in the value of excimer GP represents an increase in excimer probability.

The binding of PLA_2 to DPPC vesicles was measured either by the intensity of the enzyme's tryptophan fluorescence (excitation = 280 nm, emission = 340 nm) as described (*28*) or by resonance energy transfer between the tryptophan of the PLA_2 (donor) and the dansyl-DHPE in the vesicles (acceptor) at an emission wavelength of 510 nm. The dansyl was excited at 280 nm to measure energy transfer and at 340 nm to measure the intrinsic dansyl fluorescence. Results were evaluated as described (*16*). Energy transfer was calculated using the equation

$$\mathrm{ET} = \frac{F_{280,\max} - F_{280,i}}{F_{280,0} F_{\mathrm{PLA}_2}} \tag{3}$$

where $F_{280,\max}$ is the steady-state intensity of dansyl fluorescence (ex = 280, em = 510) in the presence of PLA_2 and $F_{280,i}$ is the extrapolated intrinsic dansyl fluorescence excited at 280 nm (*16*). The initial fluorescence of PLA_2 (F_{PLA2}) and dansyl-DHPE ($F_{280,0}$) in the absence of energy transfer was included in the calculation to normalize the data for comparison among samples. The extrapolated intrinsic dansyl fluorescence ($F_{280,i}$) was calculated from the dansyl fluorescence excited at 340 nm obtained simultaneously in each experiment as described (*16*) and accounted for changes in dansyl emission due to the presence of palmitic acid and lyso-PC.

RESULTS

Effects of Products on Bilayer Properties. Previous studies revealed that certain effects of the DPPC hydrolysis products, palmitic acid and lyso-PC, on DPPC bilayers could be observed using the fluorescent probes Prodan and Laurdan, and these effects correlated with the ability of the products to enhance PLA_2 activity (*16*, *17*). These previous studies were restricted entirely to steady-state fluorescence and mostly to equimolar combinations of the two products. To address the questions left by those studies, we have now examined the effects of each product individually and compared them to the effects observed in the presence of both products together. These comparisons have been assisted by more detailed experiments involving time-resolved fluorescence spectroscopy.

As shown in Figure 1, the Prodan and Laurdan emission spectra at 44 °C are broad and centered at about 470−480 nm. Such spectra are consistent with interactions between the probes and the water molecules in a hydrophobic environment as is expected in the liquid crystalline phase of DPPC bilayers (*16*, *17*, *27*; the main phase transition temperature of DPPC LUV is about 41.5 °C). The addition of palmitic acid caused both spectra to shift toward shorter wavelengths. The Laurdan spectrum was also narrowed and the peak intensity increased (Figure 1B). In contrast, the Prodan spectrum remained broad with two discrete peaks now resolved (Figure 1A). Also, the peak intensity was reduced by the presence of palmitic acid.

It is thought that changes in the emission spectra of Prodan and Laurdan in lipid bilayers reflect changes in dipolar relaxation due to the content and mobility of bilayer water (*27*). To further understand how palmitic acid affects the bilayer water near Prodan and Laurdan, time-resolved emission spectra were obtained. Time-dependent shifts in the spectra were visualized by plotting the spectrum center of mass as a function of time (Figure 1, parts C and D). In the control experiment with each probe, the center of mass increased rapidly over the first 2.5 ns and approached a

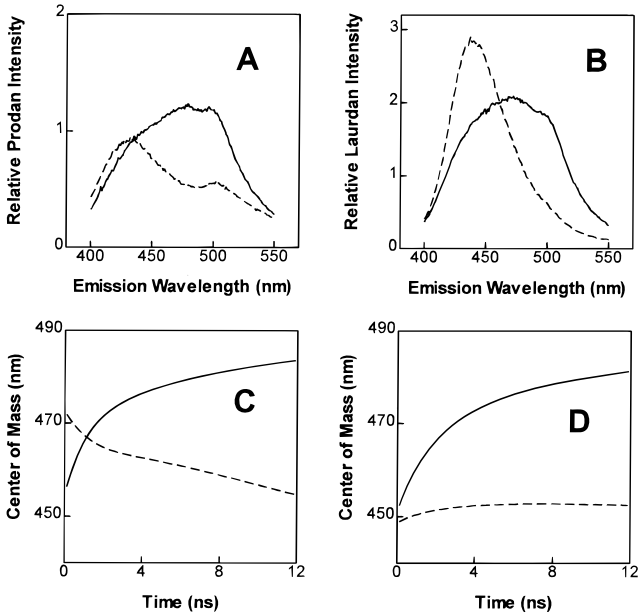

FIGURE 1: Steady-state (panels A and B) and time-resolved (panels C and D) emission spectra of Prodan (panels A and C) and Laurdan (panels B and D) in the absence (solid curves) and presence (dashed curves) of 20 mol % palmitic acid. The time-resolved spectra are displayed as the time dependence of the spectral center of mass as calculated by the Globals Unlimited software. Experimental conditions were 500 μM DPPC, about 1 μM Laurdan, 1 μM calcium, pH 8, and 44 °C. The excitation wavelength was 350 nm.

steady state by 12.5 ns. When palmitic acid was added to vesicles containing Laurdan, the center of mass increased only slightly and leveled off at approximately 450 nm, suggesting a reduction in dipolar relaxation. In contrast, when palmitic acid was added to DPPC vesicles containing Prodan, the center of mass decreased from an initial wavelength of 475 nm to approximately 450 nm. This time-dependent decrease in the center of mass was a consequence of the red part of the spectrum being dominated by a short lifetime (average lifetime at 520 nm = 2.5 ns) compared to that of the blue (average lifetime at 430 nm = 5.5 ns). Such shifts to shorter wavelength represent exposure of some of the Prodan molecules to bulk water (*29*). Thus, palmitic acid reduced the exposure of Laurdan to water but increased the exposure of a fraction of Prodan to bulk water.

The change in the Laurdan spectrum was quantified by calculating the generalized polarization (GP) value (*27*). An increase in GP indicates that the emission spectrum has shifted to shorter wavelength and is generally interpreted as signifying a decrease in polarity of the bilayer. Accordingly, the data in Figure 1B represent an increase in Laurdan GP from −0.056 to 0.641. It has been reported that palmitic acid raises the phospholipid melting temperature (t_m) (*30*, *31*). Since the results shown in Figure 1 could reflect an increase in t_m, we tested whether such was the sole effect of palmitic acid by repeating the observations of Figure 1B at various temperatures (Figure 2). The t_m can be seen in the control data (squares) by the abrupt change in the value of GP centered at about 41 °C. The addition of palmitic acid did significantly shift the t_m. However, the change in t_m does not explain all the changes in GP caused by palmitic acid since GP was still increased by palmitic acid beyond the phase-transition range, especially at temperatures above t_m.

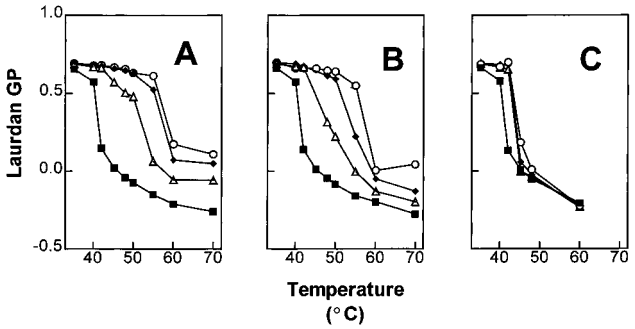

FIGURE 2: Effect of palmitic acid on Laurdan GP as a function of temperature and pH. Samples were suspended in 60 mM phosphate buffer at pH 5 (panel A), pH 7 (panel B), or pH 9 (panel C). Vesicle concentration was 91 μM DPPC (about 0.2 μM Laurdan), and palmitic acid concentrations were 0 (squares), 11 (triangles), 22 (diamonds), and 33 mol % (circles). GP was calculated from Laurdan emission intensities at 435 and 500 nm as described in the text (excitation = 350 nm).

To determine whether the changes seen in the Laurdan spectra were mediated by the protonated or unprotonated form of the palmitic acid, experiments were performed with vesicles suspended in buffer at various pH values between 3 and 9. Figure 2 shows the data obtained at pH 5, 7, and 9 as representative of the overall effect. Consistent with previous observations, palmitic acid increased the t_m of DPPC LUV best at low pH. Furthermore, the effects of palmitic acid on bilayer polarity beyond the alteration of t_m were also sensitive to pH. Since the p*K* for palmitic acid in DPPC bilayers is reported to be around 7.5−8.5 (*31*−*33*), these data suggest that effects of palmitic acid detected by Laurdan are all mediated by the protonated (uncharged) form of the fatty acid. Similar results were obtained with Prodan;[2] spectral changes were greater at pH 5 and 7 compared to pH 9 (not shown).

The pH experiments led us to the question of whether high calcium would neutralize the charge of the unprotonated palmitic acid and give the same shift in t_m as low pH. However, Figure 3A shows that the addition of calcium at pH 8 had the same effect as raising the pH. Calcium concentrations in the range of 10 μM to 1 mM greatly reduced the effects of palmitic acid on bilayer polarity. One possible explanation for the effect of calcium shown in Figure 3A is that calcium decreases the amount of palmitic acid partitioned in the bilayer. To examine that possibility, we used a fluorescent-labeled fatty acid binding protein (ADIFAB) as a monitor of the free fatty acid concentration. ADIFAB has been used for such experiments in the past to measure fatty acid partition coefficients under various experimental conditions (*15*, *34*). Importantly, calcium does not directly alter the affinity of fatty acid for ADIFAB (*15*, *34*). As shown in Figure 3B, the presence of free palmitic acid causes a large shift in the ADIFAB emission spectrum (dashed curve compared to solid curve). Addition of calcium produced a partial reversal of the shift presumably due to the reduction in free fatty acid concentration as it formed complexes with the calcium. We assumed that any changes in the bilayer partitioning of palmitic acid due to precipitation

[2] Although pH 3 behaved the same as pH 5 and 7 with Laurdan, the spectral effects of palmitic acid on Prodan were attenuated at pH 3. The reasons for this difference are not known.

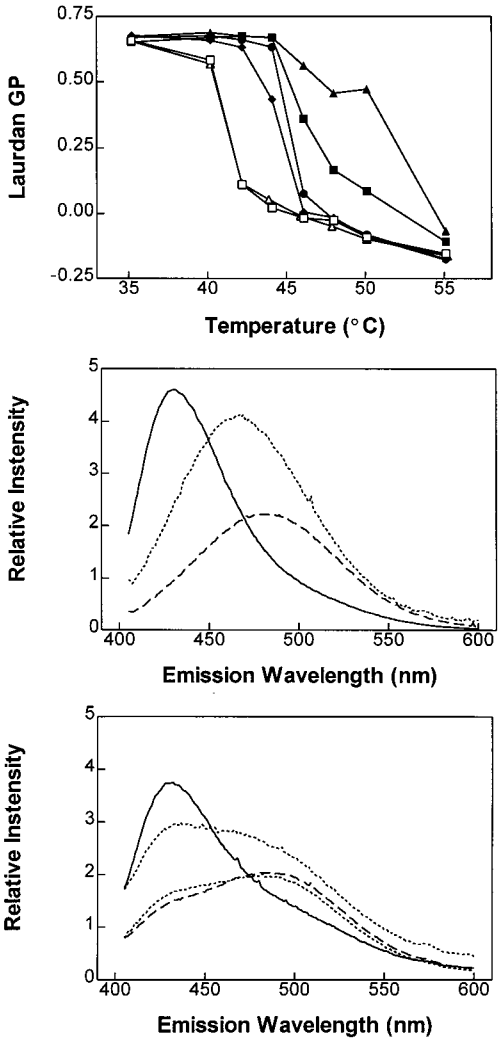

FIGURE 3: Effect of calcium on the interaction between DPPC LUV and palmitic acid. Panel A: the experiments of Figure 2 were repeated at pH 8 and 22 mol % palmitic acid at 1 μM (solid triangles), 11 μM (solid squares), 100 μM (circles) and 1 mM calcium (diamonds). Controls at 1 μM and 1 mM calcium in the absence of palmitic acid are illustrated by the open squares and open triangles, respectively. Panels B and C: The effect of 20 μM palmitic acid and subsequent addition of calcium on ADIFAB emission spectra in the absence (panel B) and presence (panel C) of DPPC (100 μM) LUV at 46 °C. The solid curves represent ADIFAB (0.2 μM) in buffer containing no additional calcium or palmitic acid. Palmitic acid (20 μM) was then added (dashed curves). The dotted curve in panel B represents 30 μM calcium. The dotted curves in panel C represent the addition of 100 μM or 1 mM calcium (from lowest to highest intensity at 450 nm). The excitation wavelength was 390 nm.

with calcium would also be reflected by alterations in the free fatty acid concentration. Thus, we repeated the experiment of Figure 3B in the presence of DPPC LUV (Figure 3C). As shown in the figure, calcium still perturbed the palmitic acid equilibrium, but only at calcium concentrations above about 100 μM. These results suggested that attenuation of palmitic acid-induced alterations of bilayer properties by calcium (Figure 3A) probably involved extraction of palmitic acid from the bilayer above 100 μM calcium and direct interactions between calcium and membrane-bound palmitic acid at lower concentrations.

The effects observed with lyso-PC were quite different from those with palmitic acid. Lyso-PC increased the polarity of the bilayer at 44 °C as shown by the shift in the

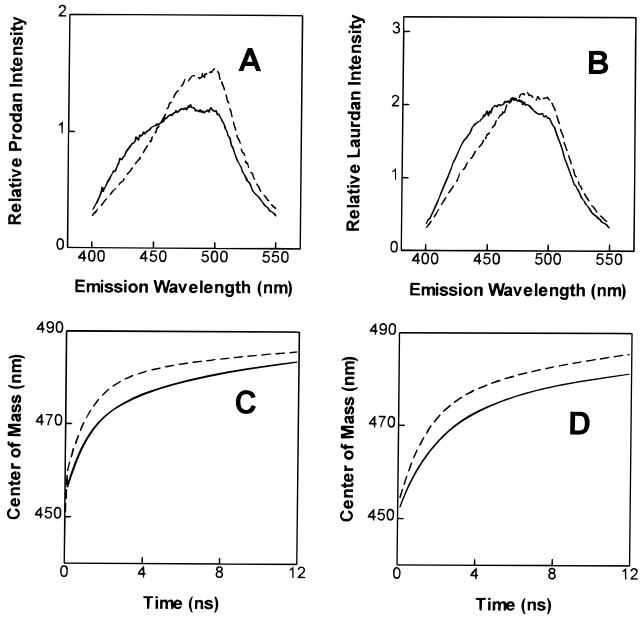

FIGURE 4: Steady-state (panels A and B) and time-resolved (panels C and D) emission spectra of Prodan (panels A and C) and Laurdan (panels B and D) in the absence (solid curves) and presence (dashed curves) of 20 mol % lyso-PC. The experimental conditions were identical to Figure 1.

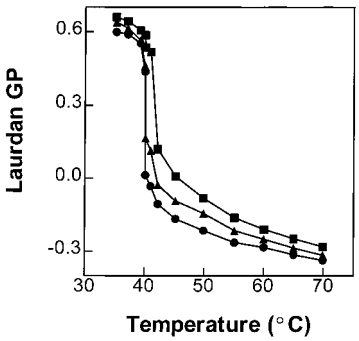

FIGURE 5: Effect of lyso-PC on Laurdan GP as a function of temperature. All samples contained 1 μM calcium and 91 μM DPPC at pH 8. Lyso-PC concentrations were 0 (squares), 11 (triangles), and 22 mol % (circles). GP was calculated from Laurdan (0.2 μM) emission intensities as in Figure 2.

Prodan and Laurdan spectra toward longer wavelength (Figure 4A and B). Also, lyso-PC caused the center of mass of Prodan and Laurdan emission spectra to increase more rapidly to an equal or higher level (Figure 4C and D). There was no evidence that lyso-PC increased the exposure of Prodan to bulk water as did palmitic acid. The same result was obtained at both high and low calcium at 44 °C.

Lyso-PC lowered the t_m of DPPC LUV slightly as seen in Figure 5. Nonetheless, the effect of lyso-PC on Laurdan GP was not confined to the phase-transition region; lyso-PC lowered the value of GP at all temperatures tested, although the response was greater at temperatures above the phase transition as was true with palmitic acid (compare Figures 2 and 5). Effects on the Prodan spectrum were qualitatively similar although of larger magnitude as reported previously (*16*, *17*).

In general, the effects of an equimolar mixture of lyso-PC and palmitic acid on Laurdan and Prodan fluorescence were intermediate between those observed with each product alone. This was best illustrated in the time dependence of

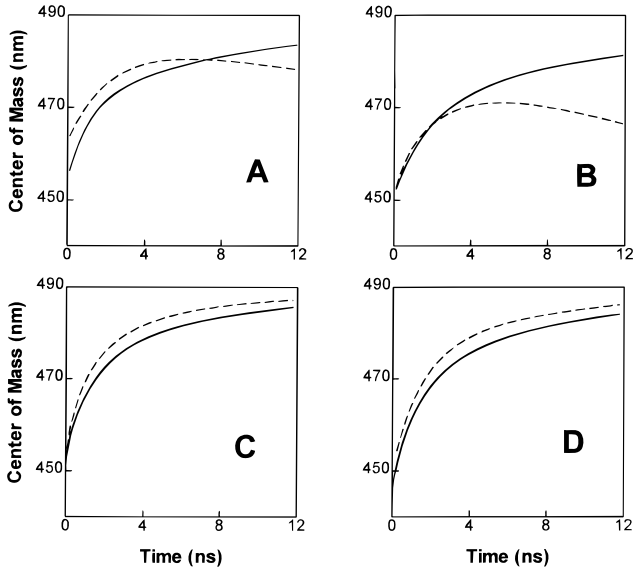

FIGURE 6: Time-resolved emission spectra of Prodan (panels A, C) and Laurdan (panels B, D) in the absence (solid curves) and presence (dashed curves) of 20 mol % each of palmitic acid and lyso-PC. The other experimental conditions were 500 μM DPPC, about 1 μM Laurdan, pH 8, 44 °C, and [calcium] = 1 μM in panels A, B; [calcium] = 1 mM in panels C, D.

the spectral center of mass (Figure 6). The relative contribution of palmitic acid or lyso-PC depended on the temperature, calcium concentration, and the probe used. As calcium concentration (panels C and D compared to A and B) increased, the influence of palmitic acid was attenuated relative to that of lyso-PC. Also, increasing the temperature from below to above t_m enhanced the relative contribution of lyso-PC consistent with prior results described for Laurdan (not shown; see ref *16*). Finally, the effect of lyso-PC appeared to dominate more with Prodan (panel A) than with Laurdan (panel B).

Effects of Products on the Binding of PLA$_2$ to the Vesicle Bilayer. The binding of PLA$_2$ to vesicles was measured in two ways: (1) by the intrinsic tryptophan fluorescence of the PLA$_2$ (*4*) and (2) by resonance energy transfer from PLA$_2$ to dansyl-DHPE (*9*, *16*). We selected two temperatures for the binding studies on the basis of the known temperature dependence of the lag phase with DPPC LUV and the *A. p. piscivorus* venom PLA$_2$ (*12*). The lag phase is longest at temperatures well below the DPPC phase transition, reaches a minimum at about 40 °C, and increases with temperature up to about 44 °C. At higher temperature, the length of the lag phase is constant with temperature. Therefore, we selected 40 and 44 °C for the remainder of the experiments.

As shown in Figure 7, the addition of palmitic acid to DPPC bilayers promotes the binding of PLA$_2$ on the basis of measurements of tryptophan fluorescence at 40 °C. This experiment was done in the absence of calcium (10 mM EDTA), confirming other observations suggesting that calcium is not required for the adsorption of PLA$_2$ to the bilayer surface (*28*, *35*). Palmitic acid was more effective at promoting binding at pH 9 than at pH 7 and 8 (Figure 7), indicating that the ionized form of the fatty acid is most responsible for increasing PLA$_2$ adsorption.

When PLA$_2$ was mixed with DPPC LUV containing dansyl-DHPE at pH 8, there was a simultaneous increase in energy transfer (triangles) and decrease in PLA$_2$ fluorescence

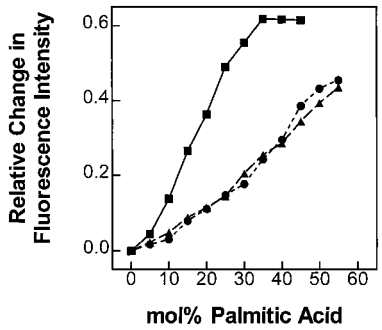

FIGURE 7: Intensity of PLA$_2$ fluorescence as a function of palmitic acid concentration in DPPC vesicles at pH 7 (circles), pH 8 (triangles), and pH 9 (squares). PLA$_2$ (5 μg/mL) was mixed with LUV (100 μM DPPC) at 40 °C with 10 mM EDTA, and the fluorescence emission at 340 nm (excitation = 280 nm) was measured following each addition of palmitic acid. The intensity is normalized to that observed prior to addition of palmitic acid.

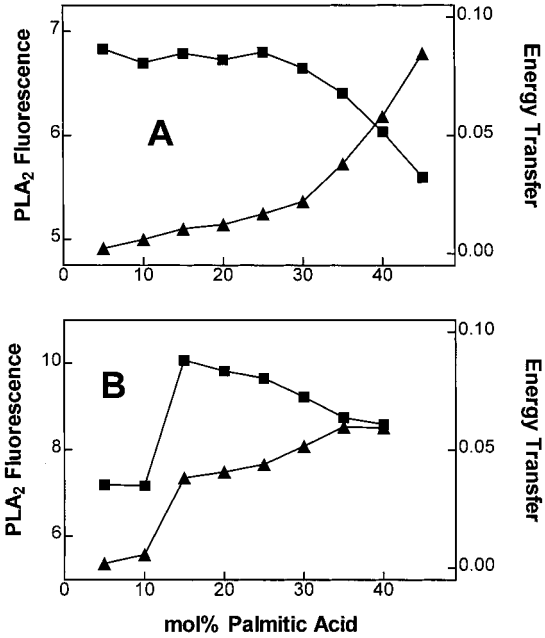

FIGURE 8: Intensity of PLA$_2$ fluorescence (squares) and resonance energy transfer (triangles) as a function of palmitic acid concentration in DPPC vesicles at pH 8 (panel A) and pH 9 (panel B). Other reaction conditions were the same as in Figure 7 except that the vesicles contained 2 mol % dansyl-DHPE. Excitation and emission wavelengths were 280 and 340 nm (squares) or 510 nm (triangles).

intensity (squares) upon palmitic acid addition (Figure 8A). In contrast, when the experiment was repeated at pH 9, the PLA$_2$ tryptophan fluorescence and dansyl fluorescence were partially uncoupled (Figure 8B). First, the amount of energy transfer to dansyl-DHPE from PLA$_2$ at high fatty acid concentration was reduced compared to lower pH (triangles), even though the data of Figure 7 demonstrated that binding of PLA$_2$ to the membrane surface is improved at pH 9. Second, at the lower concentrations of palmitic acid, the PLA$_2$ fluorescence increased as the enzyme bound to the dansyl-DHPE vesicles at pH 9 (squares, Figure 8B) instead of being quenched by energy transfer to the dansyl groups as occurred at pH 8.

Repetition of the experiments of Figures 7 and 8 with lyso-PC instead of palmitic acid revealed that lyso-PC did not increase the adsorption of PLA$_2$ to the bilayer surface in the absence of calcium. Furthermore, lyso-PC did influence the

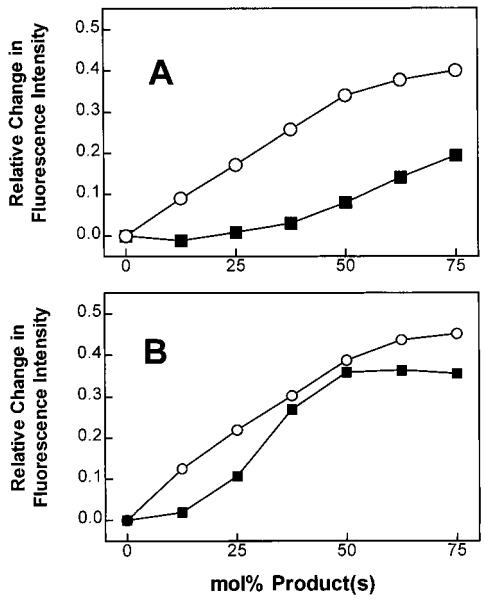

FIGURE 9: Intensity of PLA_2 fluorescence as a function of palmitic acid (circles) or equimolar concentrations of both products (squares) in DPPC vesicles at 40 °C (panel A) or 44 °C (panel B). Conditions were the same as in Figure 7 at pH 8.

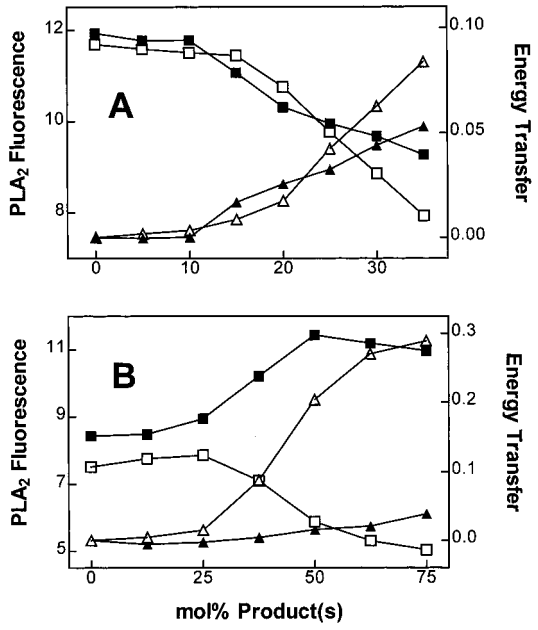

FIGURE 10: Intensity of PLA_2 fluorescence (squares) and resonance energy transfer (triangles) as a function of palmitic acid (open symbols) or equimolar concentrations of both products (solid symbols) in DPPC vesicles at 40 °C (panel A) or 44 °C (panel B). Conditions were the same as Figure 8 at pH 8.

ability of palmitic acid to promote binding. As shown in Figure 9, this influence was negative. Interestingly, the negative effect of lyso-PC on binding was less prominent at temperature above the normal DPPC phase transition (panel B). Repetition of the experiment of Figure 9 in the presence of dansyl-DHPE revealed a temperature dependence of the binding behavior. At pH 8 and 40 °C, increasing concentrations of palmitic acid (open symbols) or of a 1:1 mixture (solid symbols) quenched the PLA_2 fluorescence (Figure 10A, squares) while enhancing the dansyl fluorescence intensity (triangles). At 44 °C (panel B), palmitic acid had a similar effect (open symbols), whereas in the presence of

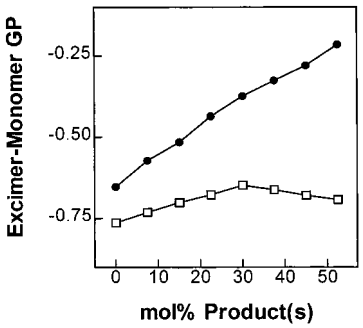

FIGURE 11: Excimer formation of pyrene-FA as a function of palmitic acid (circles) or equimolar concentrations of both products (squares) in DPPC vesicles. LUV (100 μM DPPC) were mixed with pyrene-FA (1 mol %) and the indicated concentrations of palmitic acid or palmitic acid and equimolar lyso-PC at 40 °C, pH 8, and 10 mM EDTA. GP was calculated as described in the text for monomer emission at 396 nm and excimer emission at 480 nm (excitation = 344 nm). An increase in GP indicates an increase in excimer emission.

both products, the PLA_2 and dansyl fluorescence were uncoupled (solid symbols) similar to the situation that occurred with palmitic acid at pH 9 (compare Figure 8B).

Effect of lyso-PC on the Lateral Organization of Palmitic Acid in DPPC Bilayers. Several lines of evidence suggest that the formation of bilayer heterogeneities or domains is important for promoting the membrane binding of and/or susceptibility to PLA_2 (*8*, *12*, *23*). Since the data of Figures 9 and 10 implied that lyso-PC affects this role of palmitic acid, we used measurements of the excimer and monomer fluorescence of pyrene-FA to identify possible effects of lyso-PC on the distribution of palmitic acid in the bilayer.

As palmitic acid was added to vesicles containing pyrene-FA, the value of excimer GP increased linearly, suggesting that the fatty acid became more segregated along the plane of the bilayer with each addition of palmitic acid (circles, Figure 11). When palmitic acid and lyso-PC were both added, however, the tendency for excimer formation was much less and reached a maximum at 30 mol % (squares, Figure 11). Thereafter, the value of excimer GP decreased.

Time Courses of Vesicle Hydrolysis. As shown in Figure 12A, the addition of PLA_2 to DPPC LUV (indicated by the vertical dotted line) had no effect on the fluorescence of dansyl-DHPE. This result and other related experiments have been interpreted as indicating that very low levels of PLA_2 bind to pure DPPC bilayers (*7*, *11*, *12*, *16*, *36*). At time tau, there was a substantial increase in the intensity of dansyl fluorescence excited at 280 nm, the absorption maximum of PLA_2 (curve a, Figure 12A; see also refs *12*, *16*). This increase in apparent energy transfer was accompanied by a concurrent steep decrement in intrinsic dansyl fluorescence excited at 340 nm (curve b). Control experiments studying the effects of palmitic acid and lyso-PC on dansyl emission indicated that this decrease in dansyl fluorescence was quantitatively representative of bilayer hydrolysis.

To examine the relative roles of lyso-PC and palmitic acid in contributing to this activating effect of the reaction products, we compared the individual effects of exogenously added lyso-PC and palmitic acid on the reaction time course monitoring dansyl fluorescence and energy transfer from PLA_2 to dansyl. Representative experiments at 1 μM

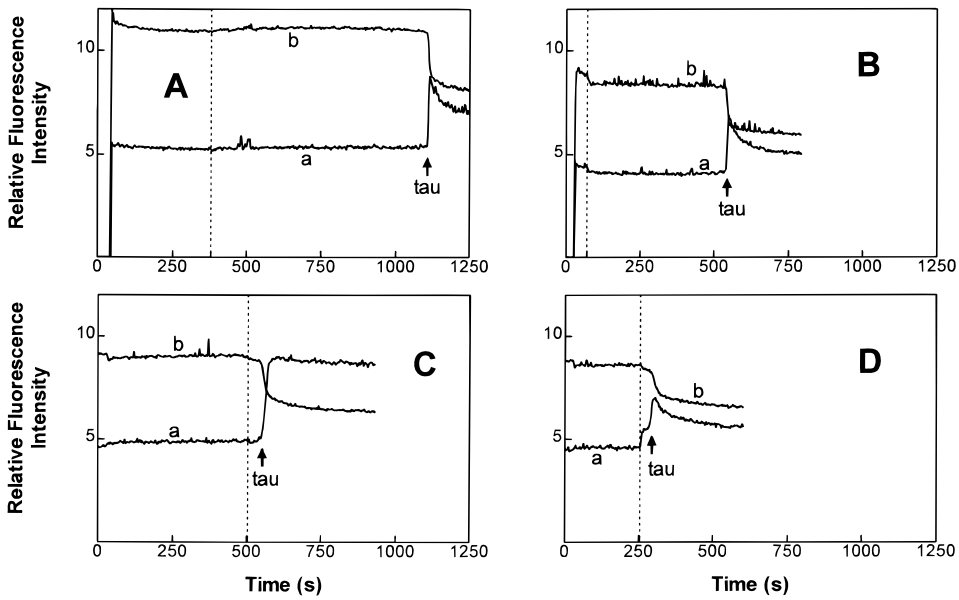

FIGURE 12: Time courses of PLA_2 binding and vesicle hydrolysis monitored by changes in resonance energy transfer from PLA_2 to dansyl-DHPE (curves a) and by decreases in the intrinsic dansyl-DHPE fluorescence intensity (curves b), respectively. PLA_2 (5 μg/mL) was added to LUV (100 μM DPPC) containing 2 mol % dansyl-DHPE at the time indicated by the vertical dotted line in each panel. The calcium concentration was 1 μM, and the temperature was 40 °C. Emission and excitation wavelengths were 280 and 510 nm for curves a and 340 and 510 nm for curves b. Added to vesicles prior to PLA_2 were the following: nothing at pH 8 (panel A), 15 mol % lyso-PC at pH 8 (panel B), 15 mol % palmitic acid at pH 7 (panel C) or 15 mol % palmitic acid at pH 9 (panel D).

calcium are shown in Figure 12B-D. To compare the effects of ionized and un-ionized palmitic acid, pH was varied in samples to which palmitic acid was added, and the results at the two pH extremes (pH 7 and 9) are shown (panels C and D).

As reported, lyso-PC was effective at reducing tau (Figure 12B; refs *10*, *11*). This reduction in tau was not accompanied by any obvious alteration in the general shape of the rise in energy transfer (curve a) or the onset of rapid hydrolysis at time tau. The addition of palmitic acid at pH 7 also shortened the lag time without altering the appearance of the events monitored by dansyl fluorescence at time tau (Figure 12C). The same result was obtained at pH 8 (not shown, but essentially identical to panel C). In contrast, repeating the experiment of Figure 12C at pH 9 gave a very different picture. In this case, energy transfer to the dansyl-DHPE was apparent immediately upon addition of PLA_2, suggesting the instantaneous binding of a significant fraction of the enzyme (curve a, Figure 12D). Nevertheless, this binding was not accompanied by bilayer hydrolysis (curve b). After a latency period (tau), the amount of energy transfer appeared to increase, and bilayer hydrolysis now occurred.

As explained previously (*11*, *12*, *15*), addition of sufficient exogenous reaction product can reduce tau to 0. The minimum concentration of product required for such to happen (X_p) has been used as an indication of the effectiveness of the products at promoting enhanced PLA_2 activity under different experimental conditions (*12*, *15*). To understand the effects of temperature and calcium on the actions of the products, X_p was measured for each reaction product and for the two products together at 1 μM and 1 mM calcium, and at 40 or 44 °C (Figure 13). A two-way analysis of variance was used to interpret the data obtained. The role of palmitic acid alone was studied only at 1 μM calcium since it does not affect tau at high calcium (*11*).

As shown in Figure 13, at 1 μM calcium, the temperature did not alter the value of X_p for either of the reaction products alone or in combination.[3] However, the presence of both products was more effective than either lyso-PC or palmitic acid alone ($p = 0.005$). X_p for lyso-PC was less in high calcium than in low at both 40 and 44 °C ($p = 0.0012$, panel B). With both products together, there appeared to be neither calcium dependence of X_p at high temperature nor temperature dependence at the low calcium concentration (panel C). However, there was a significant decrease in the value of X_p for both products at high calcium and low temperature ($p = 0.02$).

Figure 14 reveals the effect of pH (1 μM calcium) on the value of X_p. Both lyso-PC alone and both products together were slightly more effective when the pH was raised. In contrast, palmitic acid was less effective at the higher pH where it was ionized. This result suggests that whereas the ionized form of palmitic acid was better at promoting the binding of PLA_2 to the bilayer surface (Figure 7), it was less able to promote hydrolysis.

DISCUSSION

Figure 12 demonstrates that both lyso-PC and fatty acid are capable of reducing tau. As stated in the Introduction, this observation is well-documented, but the exact role of each product has not been fully established (*8*, *9*, *16*−*18*). To better clarify the mechanisms involved, we have explored the effects of each product individually and together on the kinetics of hydrolysis, the binding of PLA_2 to the bilayer

[3] The results shown for lyso-PC at low calcium and low temperature ignore several sets of data (4 of 8) in which lyso-PC was unable to reduce tau completely to 0 and no value for X_p could thus be obtained. This suggests that at low calcium, lyso-PC may be less effective at low temperature compared to high, an effect that is not revealed in the statistical analysis.

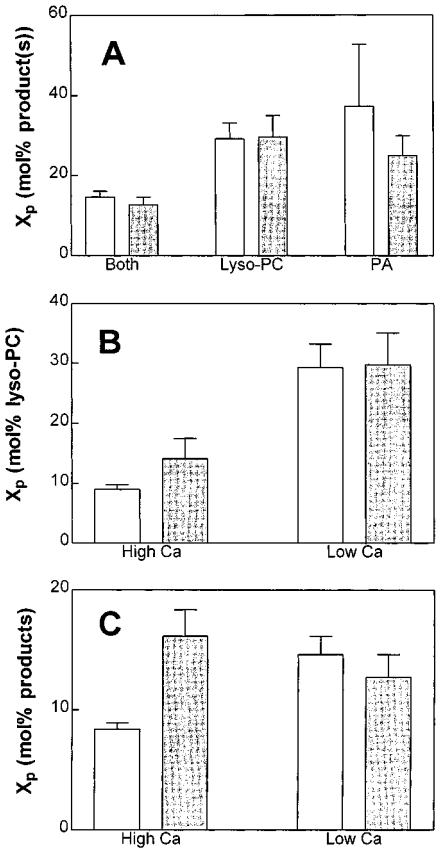

FIGURE 13: Minimum concentration of added reaction product(s) at which tau = 0 s (X_p). The calcium concentration was 1 μM ("low") or 1 mM ("high"). The temperature was 40 °C (open bars) or 44 °C (solid bars). Hydrolysis time courses such as those shown in Figure 12 were repeated under the same conditions (pH 8) with various concentrations of palmitic acid, lyso-PC, or both products (equimolar) until the threshold concentration at which a lag time before tau could not be discerned was identified (X_p). Data were analyzed by two-way analysis of variance. Error bars represent the SEM for 2−10 experiments. In panel A (low calcium), 39% of the variation in X_p was attributed to the type of reaction product added to the vesicles ($p = 0.005$). The effect of calcium concentration was responsible for 56% of the variation in panel B (lyso-PC alone added; $p = 0.0012$), and 21.5% of the variation was due to interaction between temperature and calcium concentration in panel C (both products added together, $p = 0.02$). However, neither temperature nor calcium effects were significant when considered separately.

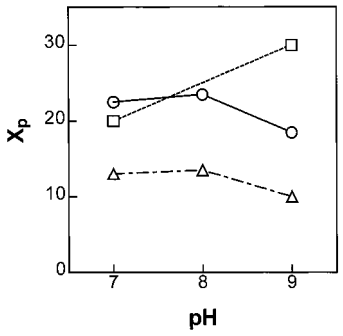

FIGURE 14: X_p for palmitic acid (squares), lyso-PC (circles), or both products together (triangles) as a function of reaction pH. X_p was determined as described for Figure 13 at the indicated pH values.

surface, and certain physical properties of the membrane known to be relevant to the action of PLA_2. The experimental design was to compare these phenomena under conditions that affect the ability of each product to reduce tau and thus to make correlations to identify specific mechanisms. The experimental conditions chosen were calcium concentration and temperature since previous work has shown that they fulfill this criterion (*12*, *15*). Also, it has generally been assumed that the effects of fatty acid on hydrolysis kinetics were due to the negative charge of the lipid (*7*−*9*, *22*, *36*). However, since the p*K* of palmitic acid in DPPC bilayers is near the pH used in most kinetic studies (i.e., pH 8, ref *31*−*33*), this assumption must be questioned. Thus, we included pH as an experimental variable in this study.

According to the data of Figure 13, the effects of temperature and calcium concentration can be summarized by three observations. First, calcium reduced the amount of lyso-PC required to induce bilayer susceptibility to PLA_2. This phenomenon is consistent with the hypothesis that lyso-PC acts at the calcium-dependent step (i.e., step two) shown in eq 1 (*20*, *28*, *35*). Second, calcium reduced the effectiveness of palmitic acid. At 1 mM calcium, lyso-PC alone was equally effective at reducing tau as both products were. As shown by the data of Figure 3, the lack of a response to palmitic acid at high calcium concentration is probably due to direct calcium/fatty acid interactions. Third, increased temperature reduced the ability of lyso-PC to shorten tau. Possible reasons for this influence of temperature are discussed below.

Surprisingly, palmitic acid was more effective at reducing tau at pH below the apparent p*K* (pH 7) than at higher pH (pH 9) where the fatty acid would be more ionized (Figure 14). This result contradicts the current dogma that the ability of fatty acid to increase bilayer hydrolysis by PLA_2 is due simply to an effect of negative charge on the binding of the enzyme (*7*−*9*, *36*). Since lyso-PC and both products together were slightly more effective at pH 9 than at pH 7 or 8, the reduced effectiveness of palmitic acid was not due to a loss of enzyme activity at high pH. Thus, the possibility must be considered that fatty acid in its un-ionized state has additional effects to promote bilayer hydrolysis. This raises two questions. (1) Why does an increase in the fraction of ionized fatty acid appear to interfere with the ability of the lipid to promote bilayer hydrolysis? (2) How might un-ionized fatty acid promote bilayer hydrolysis?

To answer the first question, we consider the pH dependence of palmitic acid-induced binding of PLA_2 to the surface of the DPPC LUV. Calcium-independent absorption of the enzyme was observed as palmitic acid was added to the vesicles both by tryptophan fluorescence (Figure 7) and by resonance energy transfer from tryptophan to dansyl-DHPE, supporting the assertion that step 1 in eq 1 does not involve calcium (*20*, *28*, *35*). When assessed by PLA_2 fluorescence (Figure 7), the ability of palmitic acid to promote binding was enhanced by increased pH as would be expected if the effect involved electrostatic interactions as proposed (*8*, *9*, *22*). Nonetheless, the energy-transfer data (Figure 8) provide a clue as to why such does not make palmitic acid more effective at promoting hydrolysis. If all PLA_2 molecules that bind to the bilayer surface transfer their excited-state energy to the dansyl-DHPE, the tryptophan fluorescence should be quenched rather than being enhanced as occurs in the absence of dansyl. Furthermore, the quenching should be symmetrical with the enhancement of energy transfer. As shown

in Figure 8A, this is what occurred at pH 8. Thus, it appeared that each PLA_2 molecule had an equal probability of contact with the dansyl-DHPE probe upon adsorption to the bilayer surface.[4] In contrast, when the experiment was repeated at pH 9 (Figure 8B), there was less energy transfer observed, even though the total amount of PLA_2 adsorbed to the bilayer surface was increased (based on the data of Figure 7). Moreover, the tryptophan fluorescence increased as fatty acid was added rather than being quenched. These results suggest that a population of the PLA_2 was binding to membrane locations without access to dansyl-DHPE at pH 9. A likely possibility is that the enzyme was binding to fatty acid-rich domains depleted of dansyl-DHPE and presumably other phospholipid molecules. Since the enzyme would be sequestered away from substrate under such conditions, this interpretation would explain why fatty acid was less effective at reducing tau at high pH even though it was more effective at promoting enzyme adsorption. Indeed, the data of Figure 12D (pH 9) demonstrated that concentrations of palmitic acid that caused an immediate increase in energy transfer between PLA_2 and dansyl-labeled phospholipid did not necessarily cause concurrent rapid hydrolysis of the vesicles. Also, Burack et al. (*9*) recently suggested that strong binding to fatty acid can be detrimental to the progress of the hydrolysis reaction by sequestering the enzyme in fatty acid-rich domains devoid of substrate and thereby causing "product inhibition" (*37*).

Additional support for this notion that fatty acid promotes hydrolysis by mechanisms beyond enhancing PLA_2 adsorption to the membrane surface was obtained using vesicles composed of the anionic phospholipid, dipalmitoylphosphatidylglycerol (DPPG). Importantly, DPPG contributes negative charge like fatty acid but does not perturb the bilayer structure as does palmitic acid. Measurements of X_p for lyso-PC or for both products together were made with DPPC vesicles containing various amounts of DPPG. Increasing concentrations of DPPG in the vesicle membrane enhance the binding of PLA_2 and reduce tau, presumably due to the negative charge (*9*). However, DPPG did not reduce the value of X_p for lyso-PC regardless of temperature or calcium concentration (based on multiple regression analysis). Thus, it appears likely that the effect of palmitic acid to lower the requirement for lyso-PC (i.e., decrease X_p as in Figures 13A and 14) and some of the effects to reduce tau (especially at pH $<$ 9) involve perturbation of the bilayer rather than accumulation of negative charge.

Thus, it is necessary to answer the second question and consider what physical changes occur in the bilayer at pH $<$9 that might explain the additional effects of palmitic acid on the hydrolysis kinetics. First, previous work has shown that fatty acid tends to segregate into domains in the bilayer and that domain formation in general appears important for promoting step 2 in eq 1 (*12*, *23*). We assessed the tendency of palmitic acid to segregate by observing the propensity of pyrene-FA in the bilayer to form excimers (*12*, *23*). Figure 11 showed that addition of palmitic acid to DPPC vesicles containing pyrene-FA increased the excimer probability, suggesting that clusters of fatty acid had formed. Identical results were obtained regardless of pH (not shown), indicating that this phenomenon occurs for both the ionized and the un-ionized forms of palmitic acid.

Second, un-ionized palmitic acid selectively caused certain physical perturbations to the bilayer revealed by the decrease in bilayer polarity sensed by both Laurdan and Prodan and the increased exposure of Prodan to bulk water. The reduced polarity probably reflects an increase in phospholipid ordering due to interactions between the fatty acid and the phospholipid acyl chains (*38*). The exposure of Prodan to bulk water could represent a decrease in Prodan partitioning resulting from Prodan being squeezed out of the bilayer by the phospholipid ordering (*39*). However, if such were the case, one might expect that the fatty acid would not cause a decrease in Prodan partitioning under conditions at which the phospholipid ordering is not observed. For example, when both products were present together at low calcium concentration, the effects of palmitic acid on phospholipid ordering and bilayer polarity were absent or greatly reduced (*16*). Nevertheless, the ground-state heterogeneity of Prodan populations was still present (Figure 6). A second explanation for the larger fraction of Prodan exposed to bulk water is that palmitic acid could be increasing the spacing between the phospholipid headgroups, the region normally occupied by Prodan (*40*). Consequently, the availability of hydrophobic environment sufficient to maintain the probe in and/or exclude bulk water from the headgroup region would be reduced by the increased spacing. This effect would be exaggerated by the formation of lipid domains. Hence, phospholipid clusters ordered by the presence of the fatty acid would produce the blue-shifted Prodan spectrum indicated by the peak centered at 430 nm in Figure 1A. In contrast, the peak centered at 500 nm would reflect Prodan exposed to the bulk aqueous phase because of the spaces in the headgroup region created by fatty acid-rich clusters.

Why, then, would these physical perturbations occur only with the protonated form of the fatty acid? Previous data suggests that the protonated form of palmitic acid descends deeper into the bilayer than does the ionized form (*41*, *42*). It has been proposed that in low pH solutions, the protonated palmitic acid forms hydrogen bonds with the phosphate groups of the phospholipid molecules (*41*). In the ionized form, however, the negatively charged palmitic acid would more likely be found higher in the membrane around the positively charged nitrogen of the phosphatidylcholine. Therefore, we suggest that un-ionized palmitic acid descends into the hydrophobic region of the bilayer where it stabilizes acyl chain interactions and thus increases bilayer order. This descent would then leave a larger void in the headgroup region and thus allow exposure of some of the Prodan to bulk water. We further hypothesize that this separation of headgroups would allow the PLA_2 active site greater access to the sn-2 bond of the phospholipids and would account for the increased activity.

While these interpretations may explain the ability of un-ionized palmitic acid to promote increased PLA_2 activity, the question arises as to whether these effects also occur in the presence of lyso-PC and thus are relevant to the ability of palmitic acid to reduce X_p for lyso-PC and to the events occurring during hydrolysis of pure DPPC vesicles when both

[4] We note that measurements of binding by tryptophan fluorescence appear more sensitive at low fatty acid concentrations than energy transfer since enhancement of the latter did not occur below 10 mol % palmitic acid at 40 °C or below 25 mol % at 44 °C (compare Figures 7 and 9 with 8 and 10).

reaction products would be generated stoichiometrically. As revealed by the data of Figure 6, the effects of both products together on the bilayer (at low calcium concentration) appear to be a combination of the individual influences of each agent rather than a unique response. Thus, we propose that the physical effects of un-ionized palmitic acid on the DPPC bilayer as well as its ability to promote susceptibility of that bilayer to PLA_2 occur both in the presence and absence of lyso-PC.

We consider now the role of lyso-PC. It has been hypothesized that lyso-PC promotes increased PLA_2 activity by enhancing step 2 (*17*). This suggestion was based on the assumption that step 1 involved mostly electrostatic interactions for which lyso-PC would offer no advantage over DPPC. Furthermore, it was imagined that the bilayer structural changes induced by lyso-PC would be more likely to increase the ability of substrate molecules to gain access to the enzyme active site rather than to directly enhance adsorption to the bilayer surface. Our experiments reported here provide further and more direct evidence to support these suggestions. First, in contrast to palmitic acid and as predicted, lyso-PC did not promote PLA_2 binding in the absence of calcium. Second, observation of the effects of lyso-PC on time-resolved and steady-state Prodan and Laurdan emission spectra (Figure 4) substantiated fundamental observations regarding the effects of lyso-PC on the bilayer. The increased rate and magnitude of shift of the spectral centers of mass are consistent with an increase in the rate of dipolar relaxation and/or exposure to water. This result and the observation that Prodan (located more superficially in the bilayer) was affected more than Laurdan are consistent with the interpretation that lyso-PC increases bilayer curvature, making it easier for the enzyme active site to gain access to phospholipid molecules in the membrane. Third, less lyso-PC was required to promote bilayer hydrolysis when calcium concentration was increased (Figure 13; ref *15*), consistent with a role for both agents on the same step (i.e., step 2; also see below).

Nonetheless, the data in Figures 9 and 10 indicate that lyso-PC also influences step 1 by inhibiting the ability of palmitic acid to enable PLA_2 to bind to the bilayer. Rather than being harmful as one might suppose intuitively, the modest attenuation of binding may actually promote hydrolysis by tempering the detrimental effect of the fatty acid to sequester the enzyme away from substrate. Since palmitic acid domains appear to be important for the fatty acid to foster binding (*8*, *23*), this unexpected effect of lyso-PC to suppress binding may relate to alterations in domain structure as shown in Figure 11. In contrast to the monotonic increase in apparent domain probability observed with palmitic acid alone (up to at least 50 mol %), the data with both palmitic acid and lyso-PC suggested that the pyrene-FA was maximally segregated into domains at 30 mol % palmitic acid. Further increases in palmitic acid concentration apparently increased the size of those domains and thus diluted the surface concentration of pyrene-FA. Also, the overall probability of excimer formation was reduced by lyso-PC since the value of excimer GP was less at all palmitic acid concentrations in the presence of lyso-PC. Thus, lyso-PC altered the structure of the fatty acid domains possibly by increasing their size and/or by inducing mixing. It should be noted that changes in bilayer fluidity can also affect excimer probability by altering the rate of probe diffusion. However, this cannot explain either the increase in excimer formation upon addition of palmitic acid or the effect of lyso-PC. Palmitic acid causes the bilayer to become more ordered at 40 °C (Figure 2) which would reduce excimer GP rather than raising it if changes in probe diffusion rates were responsible for the data. Likewise, the bilayer appeared to be more fluid at 40 °C in the presence of both lyso-PC and palmitic acid compared to palmitic acid alone (Figure 5), which would mean that lyso-PC should increase excimer GP if diffusion were the primary issue. Of course, this interpretation of these data assumes that pyrene-FA behaves similarly to the palmitic acid in terms of its distribution along the bilayer plane.

A question that remains is the temperature dependence of the effectiveness of lyso-PC shown in Figure 13. As shown in panel C, more reaction products were required to induce high PLA_2 activity at 44 °C than at 40 °C when calcium concentration was high ($p = 0.02$). Under such conditions, palmitic acid made essentially no contribution to the hydrolysis kinetics (as described above). Thus, lyso-PC appeared less effective at temperatures above the bilayer phase transition. A similar response appeared to occur when lyso-PC was added alone (panel B), although the effect was not statistically significant in the two-way analysis of variance presumably because the effect of calcium was so large; that is, the proportion of total variance contributed by the effect of temperature was much smaller than the effect of calcium. These results are consistent with a previous report (*12*), but it was not known until now that the effect is confined to high calcium concentration.

An explanation that has been suggested for this temperature dependence is that the bilayer dissipates the perturbation caused by lyso-PC into deeper regions of the membrane at higher temperatures, thus reducing the surface perturbations that help induce membrane susceptibility (*16*). A second explanation offered by the data reported here is that the higher temperature increases the sequestering of bound enzyme by the products, thereby offsetting some of their useful effects. Evidence for this was demonstrated in Figure 10. The binding of PLA_2 seemed homogeneous with palmitic acid alone (pH 8) at either temperature or in the presence of lyso-PC below the DPPC phase transition since the quenching of PLA_2 and enhancement of dansyl fluorescence were symmetrical in each of these cases. In contrast, different populations of bound PLA_2, some in proximity to dansyl-DHPE and some sequestered from the energy-transfer acceptor, appeared to exist when both products were added at temperatures above the phase transition. Although this effect of lyso-PC on binding was observed here in the absence of calcium, it appears to relate to effects of the lysophospholipid at high calcium concentration as well. Previously, we also observed that the amount of PLA_2 binding assessed by energy transfer to dansyl-DHPE at time tau during vesicle hydrolysis decreased at temperatures above t_m (10 mM calcium; ref *16*). In contrast, more recent analysis of the total binding of PLA_2 to DPPC vesicles (no dansyl-DHPE) by the intensity of intrinsic tryptophan fluorescence at time tau revealed no effect of temperature (not shown). Therefore, the apparent decrement in binding identified at high calcium with energy-transfer experiments probably reflected the same sequestration phenomenon displayed in

Figure 10B.

Although one or both of these phenomena may explain at least some of the influence of temperature on X_p (and thus on tau) at high calcium concentration, they do not account for the similar temperature dependence of tau at low calcium (*12*, *16*, *43*). This effect of temperature on tau at low calcium may be rationalized by considering the structural fluctuations between domains of gel and liquid crystalline states in the bilayer that occur at temperature near t_m. These fluctuations have been hypothesized to create defects in the bilayer that help activate PLA_2 (*43*, *44*). If this is true, it would help explain why tau has been found to be smallest at the phase transition where the frequency of fluctuation is greatest.

Last, the results of this study help to resolve some of the mysteries that have remained regarding the effects of the calcium on hydrolysis kinetics. Although it is well-known that calcium is an obligatory cofactor for the low molecular weight soluble PLA_2, additional effects of the cation to decrease X_p and alter the physical effects of the reaction products on the bilayer have been reported (*15*, *16*). For example, reaction products lower the DPPC t_m at high but not low calcium concentration, and the value of Laurdan GP is elevated at temperatures above t_m at low but not high calcium (*16*). These kinetic and physical effects of calcium were not interpreted in the past but now appear easily explained by considering the following observations identified in the data of this paper. First, the physical effects of both reaction products on the DPPC bilayer appear to reflect a combination of the individual influence of each product alone (Figure 6). Thus, by considering the behavior of each as a function of calcium concentration, one should be able to rationalize the effects of equimolar concentrations of both. Second, lyso-PC and palmitic acid caused essentially opposite changes to the DPPC t_m and bilayer polarity (Figures 2, 4, and 5). Third, the action of palmitic acid was reduced by the presence of calcium apparently through interactions between the lipid and cation in the bilayer at calcium concentrations below about 100 μM and through extraction of the fatty acid from the bilayer at higher calcium (Figure 3). Fourth, calcium did not alter the physical effects of lyso-PC on the vesicle membrane. Fifth, calcium enhanced the influence of lyso-PC on the kinetics of bilayer hydrolysis by PLA_2 (Figure 13), presumably because both molecules promote the same step (step 2) described in eq 1. Thus, increasing calcium concentration (even in the micromolar range) shifts the physical effects of reaction products on the bilayer from behavior reflecting an approximately equal contribution of both lipids to that essentially identical to the action of lyso-PC alone (Figures 4 and 6). Likewise with reaction kinetics, calcium had a strong effect on X_p for lyso-PC alone, but that effect was compensated by the contribution of palmitic acid at low calcium when both products were used (Figure 13C). The only alteration of X_p remaining with both reaction products was the effect of temperature at high calcium which appeared to reflect solely the temperature dependence of lyso-PC on reaction kinetics described above.

In summary, we have verified that fatty acid does promote calcium-independent PLA_2 binding electrostatically and that lyso-PC enhances bilayer susceptibility physically. More significantly, we have identified two novel roles for these reaction products: attenuation of fatty acid-induced binding by lyso-PC and enhancement of membrane susceptibility by un-ionized fatty acid. These conclusions are summarized by the following adaptation of eq 1

$$E + V \underset{\substack{\uparrow FA^- \\ \downarrow lyso\text{-}PC}}{\rightleftharpoons} E_B \overset{Ca^{2+}}{\underset{\substack{\uparrow FA \\ \uparrow lyso\text{-}PC}}{\rightleftharpoons}} E_B^* \qquad (4)$$

where FA^- and FA denote the ionized and un-ionized forms of palmitic acid, respectively, and the arrows indicate whether the step is enhanced (up) or inhibited (down) by the specified reaction product.

ACKNOWLEDGMENT

We gratefully acknowledge Enrico Gratton, Theodore Hazlett, and the rest of the staff at the Laboratory for Fluorescence Dynamics (University of Illinois, Urbana, Illinois) for their assistance and the use of facility resources in generating and interpreting the fluorescence lifetime data. We also appreciate the technical assistance of Marilyn Baker, Jill Bergeson, Matthew Hyde, Chloe Maycock, Richard Orgill, James Ricks, and Michael Smith.

REFERENCES

1. Mayer, R. J., and Marshall, L. A. (1993) *FASEB J. 7*, 339−348.
2. Vadas, P., and Pruzanski, W. (1993) *Circ. Shock 39*, 160−167.
3. Vadas, P., Browning, J., Edelson, J., and Pruzanski, W. (1993) *J. Lipid Mediators 8*, 1−30.
4. Bell, J. D., and Biltonen, R. L. (1989) *J. Biol. Chem. 264*, 12194−12200.
5. Menashe, M., Romero, G., Biltonen, R. L., and Lichtenberg, D. (1986) *J. Biol. Chem. 261*, 5328−5333.
6. Lichtenberg, D., Romero, G., Menashe, M., and Biltonen, R. L. (1986) *J. Biol. Chem. 261*, 5334−5340.
7. Jain, M. K., Rogers, J., Jahagirdar, D. V., Marecek, J. F., and Ramirez, F. (1986) *Biochim. Biophys. Acta 860*, 435−447.
8. Jain, M. K., Yu, B.-Z., and Kozubek, A. (1989) *Biochim. Biophys. Acta 980*, 23−32.
9. Burack, W. R., Gadd, M. E., and Biltonen, R. L. (1995) *Biochemistry 34*, 14819−14828.
10. Jain, M. K., and De Haas, G. H. (1983) *Biochim. Biophys. Acta 736*, 157−162.
11. Bell, J. D., and Biltonen, R. L. (1992) *J. Biol. Chem. 267*, 11046−11056.
12. Bell, J. D., Baker, M. L., Bent, E. D., Ashton, R. W., Hemming, D. J. B., and Hansen, L. D. (1995) *Biochemistry 34*, 11551−11560.
13. Apitz-Castro, R., Jain, M. K., and De Haas, G. H. (1982) *Biochim. Biophys. Acta 688*, 349−356.
14. Gheriani-Gruszka, N., Almog, S., Biltonen, R. L., and Lichtenberg, D. (1988) *J. Biol. Chem. 263*, 11808−11813.
15. Bent, E. D., and Bell, J. D. (1995) *Biochim. Biophys. Acta 1254*, 349−360.
16. Bell, J. D., Burnside, M., Owen, J. A., Royall, M. L., and Baker, M. L. (1996) *Biochemistry 35*, 4945−4955.
17. Sheffield, M. J., Baker, B. L., Li., D., Owen, N. L., Baker, M. L., and Bell, J. D. (1995) *Biochemistry 34*, 7796−7806.
18. Burack, W. R., Dibble, A. R. G., Allietta, M. M., and Biltonen, R. L. (1997) *Biochemistry 36*, 10551−10557.
19. Scott, D. L., White, S. P., Otwinowski, A., Yuan, W., Gelb, M. H., and Sigler, P. B. (1990) *Science 250*, 1541−1546.
20. Jain, M. K., Yu, B.-Z., and Berg, O. G. (1993) *Biochemistry 32*, 11319−11329.
21. Gelb, M. H., Jain, M. K., Hanel, A. M., and Berg, O. G. (1995) *Annu. Rev. Biochem. 64*, 653−688.
22. Han, S. K., Yoon, E. T., Scott, D. L., Sigler, P. B., and Cho, W. (1997) *J. Biol. Chem. 272*, 3573−3582.
23. Burack, W. R., Yuan, Q., and Biltonen, R. L. (1993) *Biochemistry 32*, 583−589.

24. Maraganore, J. M., Merutka, G., Cho, W., Welches, W., Kézdy, F. J., and Heinrikson, R. L. (1984) *J. Biol. Chem. 259*, 13839−13843.
25. Bartlett, G. R. (1959) *J. Biol. Chem. 234*, 466−468.
26. Bhamidipati, S. P., and Hamilton, J. A. (1995) *Biochemistry 34*, 5666−5677.
27. Parasassi, T., De Stasio, G., Ravagnan, G., Rusch, R. M., and Gratton, E. (1991) *Biophys. J. 60*, 179−189.
28. Bell, J. D., and Biltonen, R. L. (1989) *J. Biol. Chem. 264*, 225−230.
29. Krasnowska, E. K., Gratton, E., and Parasassi, T. (1998) *Biophys. J.* (in press).
30. Schullery, S. E., Seder, T. A., Weinstein, D. A., and Bryant, D. A. (1981) *Biochemistry 20*, 6818−6824.
31. Fernández, M. S., González-Martínez, M. T., and Calderón, E. (1986) *Biochim. Biophys. Acta 863*, 156−164.
32. Ptak, M., Egret-Charlier, M., Sanson, A., and Bouloussa, O. (1980) *Biochim. Biophys. Acta 600*, 387−397.
33. Cevc, G., Seddon, J. M., Hartung, R., and Eggert, W. (1988) *Biochim. Biophys. Acta 940*, 219−240.
34. Richieri, G. V., Ogata, R. T., and Kleinfeld, A. M. (1992) *J. Biol. Chem. 267*, 23495−23501.
35. Yu, B., Berg, O. G., and Jain, M. K. (1993) *Biochemistry 32*, 6485−6492.
36. Jain, M. K., Egmond, M. R., Verheij, H. M., Apitz-Castro, R., Dijkman, R., and De Haas, G. H. (1982) *Biochim. Biophys. Acta 688*, 341−348.
37. Kupferberg, J. P., Yokoyama, S., and Kèzdy, F. J. (1981) *J. Biol. Chem. 256*, 6274−6281.
38. Pauls, K. P., MacKay, A. L., and Bloom, M. (1983) *Biochemistry 22*, 6101−6109.
39. Zeng, J., and Chong, P. L.-G. (1995) *Biophys. J. 68*, 567−573.
40. Chong, P. L.-G., and Wong, P. T. T. (1993) *Biochim. Biophys. Acta 1149*, 260−266.
41. Barratt, M. D., and Laggner, P. (1974) *Biochim. Biophys. Acta 366*, 127−133.
42. Abrams, F. S., Chattopadhyay, A., and London, E. (1992) *Biochemistry 31*, 5322−5327.
43. Hønger, T., Jørgensen, K., Biltonen, R. L., and Mouritsen, O. G. (1996) *Biochemistry 35*, 9003−9006.
44. Burack, W. R., and Biltonen, R. L. (1994) *Chem. Phys. Lipids 73*, 209−222.

BI9728809